

Vacuum Chamber Design of NSLS-II Storage Ring

L. Doom, M. Ferreira, H.C. Hseuh, F. Lincon, C. Longo, V. Ravindranath, S. Sharma
National Synchrotron Light Source II Project, Brookhaven National Laboratory
Upton, NY, 11973-5000 USA

Abstract

National Synchrotron Light Source II (NSLS II) will be a 3-GeV, 792-meter circumference, 3rd generation synchrotron radiation facility, with ultra low emittance and extremely high brightness. The storage ring has 30 Double-Bend-Achromatic (DBA) cells. In each cell, there are five magnets and chamber girders, and one straight section for insertion devices or Radio Frequency (RF) cavities or injection. Most vacuum chambers are made from extruded aluminum with two different cross sections: one fitted in the dipole magnets, and the other surrounded by multipole magnets. We discuss the layout of the DBA cells, the detailed design of the cell's vacuum chambers, the mounting of the Beam-Position-Monitor (BPM) buttons, discrete absorbers, lumped pumps and the distributed Non-Evaporable Getter (NEG) strips, and describe the fabrication and testing of these prototype cell chambers. Our account also details the development of the chamber bakeout process, the NEG strip's supports, and the RF shielded bellows.

1. Introduction

The National Synchrotron Light Source (NSLS), a 2nd generation synchrotron radiation facility at Brookhaven National Laboratory, has provided high flux photon beams from IR to hard X-ray for several thousand users annually since 1982. It consists of two storage rings, an 800-MeV, 1000 mA VUV ring, and a 2.8-GeV x 300-mA X-ray ring. However, the NSLS has reached the theoretical limits of its performance given its small circumference, small periodicity, and the small number of insertion devices possible. It is imperative to build a new storage ring, such as the NSLS-II combining extremely high brightness, flux, and stability, to better serve the user community and enable the exploration of the scientific challenges faced in developing new materials with advanced properties. The NSLS-II will be a 3-GeV, 500 mA storage ring, delivering photons with average spectral brightness in the 2 keV to 10 keV energy range exceeding 1021 ph/mm²/mrad²/s/0.1%BW [1]. Such cutting-edge performance requires a storage ring that will support a very high-current electron beam with horizontal emittance down to 0.6 nm-rad and vertical emittance < 8 pm-rad. The stability of the electron beam must be assured: its position (<10% of its size), angle (<10% of its divergence), dimensions (<10%), and intensity ($\pm 0.5\%$ variation). The 792 m circumference 3-GeV storage ring consists of 30 double bend achromatic (DBA) cells, with alternating straight sections, 6.6 m and 9.3 m long, bracketing each cell. This ring is intended to be a versatile light source of hard- and soft-X-rays from ~ 10 eV to ~ 20 keV with average spectral brightness and flux 10,000 times higher than those of the NSLS, and significantly exceeding all currently operating synchrotron light sources, and those under construction. Meeting this unprecedented performance entails extreme stability and alignment requirements for all the lattice magnets and beam position monitors (BPM). Figure 1 is a 3-D model of a DBA cell; it consists of two bending magnet girders and three girders for multipole magnets in the arc and matching sections. Three 9.3 m long straight sections of the 30 straight sections will be used for injection and for RF systems; therefore, 27 straight sections will be available for insertion devices. The NSLS-II will accommodate a variety of different types of undulators and wigglers that will generate high-brightness and high-flux beams of hard- and soft-X-rays. From its first day of operation, three types of insertion devices will be available for experimenters; damping wigglers providing the highest flux broadband radiation from 5 keV to 30 keV, elliptically polarized undulators offering circular- and linear-polarized soft x-ray radiation, and mini-gap in-vacuum undulators delivering high-brightness hard X-rays from 2 keV to 20 keV. In combination with bend-magnet radiation, the three-pole wigglers will be inserted just

upstream of the end of second bending magnets to provide 30 more bend-magnet-like sources of hard X-ray radiation up to 25 keV. Therefore a minimum of 57 beam lines of intense X-ray radiation will be available.

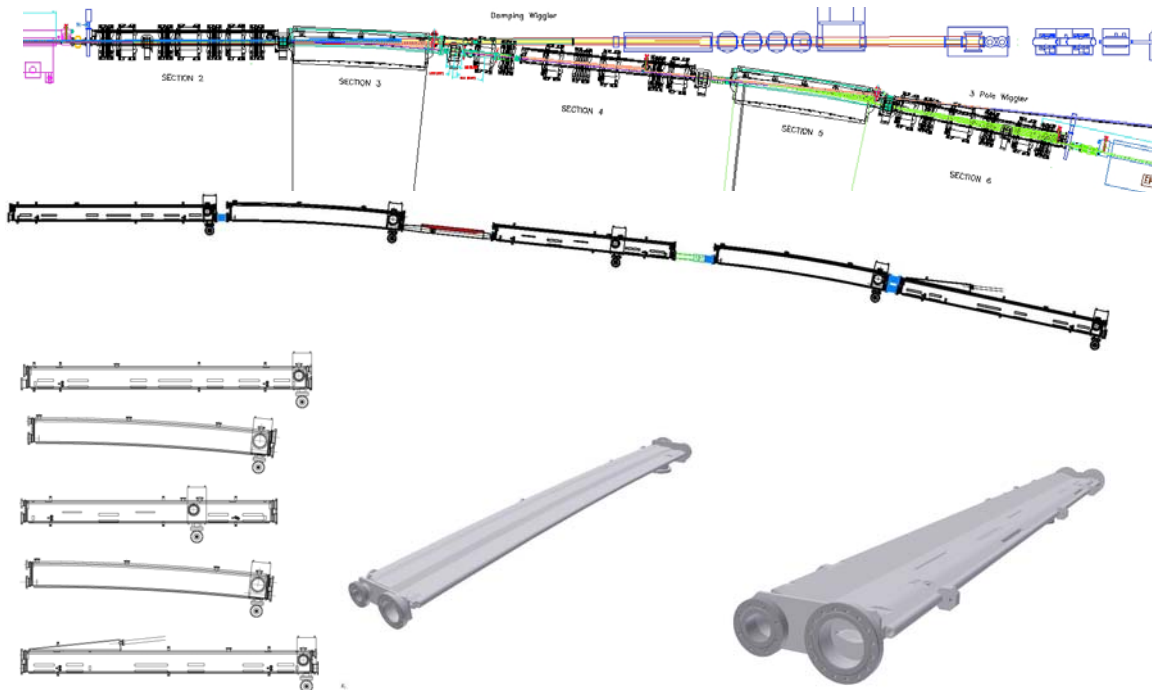


Figure 1. Layout of the five DBA cell magnets and girders (top) and the bare vacuum chambers (middle), showing the five extruded aluminum vacuum chambers, the two short stainless-steel chambers, four RF-shielded bellows and the two photon exit ports. The individual chambers are shown at the bottom, with five cell aluminum chambers, and the 3-D models of the dipole and multipole chamber. The chambers are made from aluminum extrusion, with an electron beam channel at the right side, and the antechamber at the left.

2. Vacuum Chamber: Design and Fabrication

There are multiple choices for designing the chamber and selecting material suitable for 3rd generation light source storage ring, with those chosen mostly depending on the machine's parameters, previous experience and cost. Aluminum was chosen as the cell-chamber material for the NSLS-II based on our experience, its vacuum and mechanical properties, ease of machining it, and the reasonable cost of its fabrication. With aluminum, no conductive coatings or strips are needed to reduce the impedance of the chamber's wall. A major difference between the NSLS-II and other new synchrotron radiation facilities of comparable energy is the former's lower bending field and larger bending magnet radius. The photon fan from each bending magnet will have a small dispersion and relatively low power of 2.4 kW at the full built-up current of 500 mA, which the discrete absorbers can readily intercept. This feature facilitates a narrow chamber geometry design, and thus, the cell chambers can be made from extruded aluminum of uniform cross-sections. The need to accommodate the distributed non-evaporable getter (NEG) pumping also favors using extruded aluminum, since an antechamber easily is produced by extrusion. Figure 2 illustrates the cross sections for the dipole and multipole chamber extrusions; they are similar to those of the 7-GeV Advanced Photon Source (APS) [2]. The horizontal widths of the dipole and multipole extrusions are 319,1 mm and 280,5 mm, respectively. The electron beam channels have an elliptical cross section of 25 mm (V) x 76 mm (H) offering an ample aperture for the passage of the electron beam. The size of the antechambers provides space for mounting two NEG strips top and bottom, leaving satisfactory clearance for the photon fans. The photon exit slots connecting the beam

channel and antechamber are as large as possible to provide an adequate aperture for photon fans and sufficient for vacuum-pumping conductance. However, the outside vertical height of this slot is restrained by the magnet's pole gaps, while the dimension of the inside gap is determined by the required wall thickness under the atmospheric pressure load when the chamber is under vacuum. The multipole magnets also confine the horizontal dimensions of the multipole chamber at the antechamber side. After their extrusion, the dipole chambers will be curved with rollers to the required 25 m bending radius, then the top and bottom walls of the beam's channel machined flat to a vertical height of 31 mm to fit into the 35 mm magnet gap. The dipole beam's channel has a minimum thickness of 3 mm at its top/bottom wall.

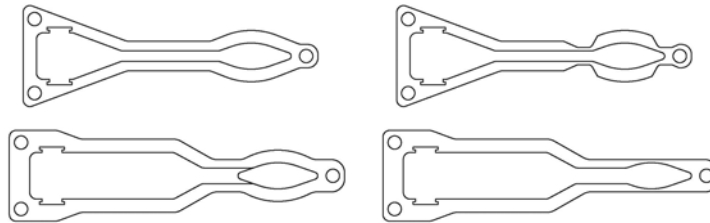


Figure 2. The extruded cross sections for multipole and dipole chambers (left); and their cross sections after machining at the magnet pole locations (right).

The multipole extrusion is machined at the quadrupole and sextupole pole locations to allow us to use magnets with smaller pole radii, while still maintaining a nominal clearance of 2 mm between the chamber wall and magnet poles for fabrication tolerance and aligning the chambers and BPMs. The minimum wall thickness at the sextupole pole locations is 3.1 mm. Finite element analysis of a multipole chamber at sextupole locations gives a maximum stress below 64 MPa, i.e., a safety factor of > 2 toward the yield strength of 145 MPa for extruded aluminum A6063. The maximum deflection at the photon exit slots at the sextupole is $< 0.3 \text{ mm} \times 2$, an acceptable value.



Figure 3. The welding of the end plates and flanges to the machined extrusions, the machined extrusion end (a), the reverse side, and the flange side of the end plate, with Conflat flanges welded, the extrusion chamber, and CAD view of a multipole chamber.

The extrusion ends are precision-machined so they can be welded smoothly to the end plates using the robotic welding machine at the APS vacuum facility, which was established specifically for producing APS vacuum chambers. Ports for absorbers, pumps, vacuum instruments, and the BPMs also are precision-machined. Figure 3 shows the sequence of welding and assembling the end plates and

flanges. All the components are chemically cleaned at the APS immediately before welding. Bi-metal explosively bonded aluminum-to-stainless Conflat flanges are welded to the end plates and side ports

3. Photon Absorbers

After welding, the chambers are assembled with photon absorbers, BPM, NEG strips, sputter ion pumps, titanium-sublimation pumps and vacuum gauges. Each DBA cell has, a total of eight water-cooled GlidCop photon-absorbers to intercept the un-used bending magnet photons, and thus protect the un-cooled flanges and bellows. These absorbers are inserted into the electron-beam's channel from the side port through the antechamber and photon exit slot into the electron beam channel. Figure 4 shows two types of bending magnet absorbers. The crotch absorbers are located at the end of the bending magnet chambers with their center opening to allow the usable photon fan to travel down the photon exit port to front end and beam line. The stick absorbers are located at the straight chambers to trim the bending magnet fan and protect the downstream un-cooled flanges, bellows and gate valves. We employed detailed ray tracing to determine the most effective locations for the absorbers without impinging into the dynamic aperture of the electron beam. Most absorbers are located 25 mm from nominal center of the beam's channel; however, to be effective, a few have to be at 22 mm and 27 mm. Due to a relatively low radiation power of 2.4 kilowatt from each bending magnet, photons are intercepted at normal incidence. The crotch absorbers intercept ~ 1.4 -kilowatt heat, while the stick absorbers each intercept less than 700 watts each. Using finite element analysis, we calculated the maximum power density and temperature at the tip of the absorbers as $< 12 \text{ W/mm}^2$ and $< 200 \text{ }^\circ\text{C}$, respectively, well within the maximum allowable temperature of $400 \text{ }^\circ\text{C}$ for GlidCop.

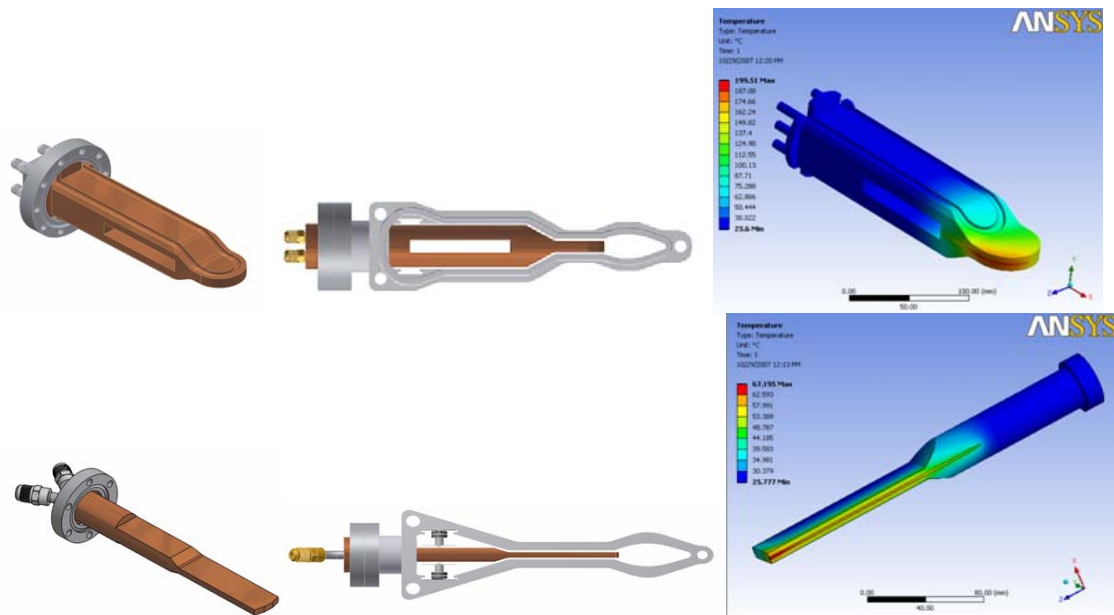


Figure 4 The 3-D models of crotch and stick absorbers (left), their positioning in the bending and multipole chambers (center), and the finite element analysis (right).

4. Beam Position Monitor

The BPMs will be installed in the machined BPM ports, where Helicoflex Delta seals will be employed to seal the feedthrough flanges onto the polished surface of the aluminum chamber. There are extreme stability and alignment requirements for all the lattice magnets and BPMs. The latter, mounted on the beam chambers must be aligned to within $\pm 30 \mu\text{m}$. The pre-aligned girders then will be moved into the ring tunnel, and installed. The required alignment tolerance between the girders is $< 100 \mu\text{m}$. The stability of their BPM vertical positions of $< \pm 0.2 \mu\text{m}$ over a few hours is preserved by controlling the tunnel's temperature to within $\pm 0.1 \text{ }^\circ\text{C}$. To achieve this accuracy, the vacuum chambers will be

supported at the BPM locations with Invar stands that have very low linear coefficient of thermal expansion. The optimum diameter of the BPM buttons is calculated to be 10 mm, and the pair must be separated by 15 mm. Figure 5 is a conceptual view of the vacuum chamber's BPMs and the feedthrough.

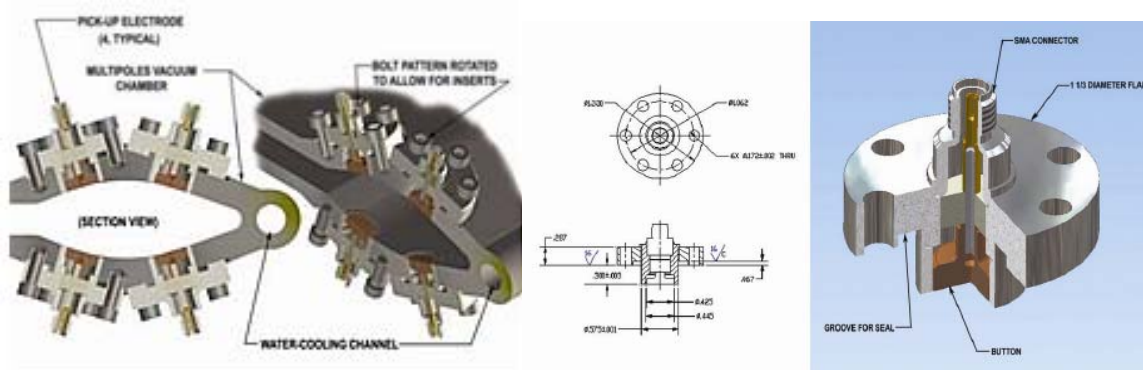


Figure 5 Four button, two-plane pick-up electrodes mounted on the chamber (left), and the designed of the feedthrough and buttons for the storage ring BPM (right).

5. Vacuum chamber bakeout

The completed cell chambers with absorbers, BPM and pumps will be assembled into the cell magnets/girder for precision alignment. Each chamber will be baked to 120 °C to ensure the integrity of the vacuum before its installation in the tunnel. After installation, all the vacuum cells again will be baked *in-situ*. The thermal outgassing of unbaked aluminum is higher than stainless steel, but an *in-situ* baked aluminum surface has outgassing rate $\leq 1 \times 10^{-12}$ Torr.liter/sec.cm². The bakeout of the storage ring cell will be accomplished by heater tapes installed along the space in between magnets under aluminum and/or kapton foil insulation, as shown in Figure 6. Additional heating jackets, heating tapes, and thermal insulation are needed for large appendaged components, such as gate valves, and ion pumps to ensure a uniform temperature distribution, especially at large flange joints where uneven temperatures may cause the seals to fail and vacuum leaks.

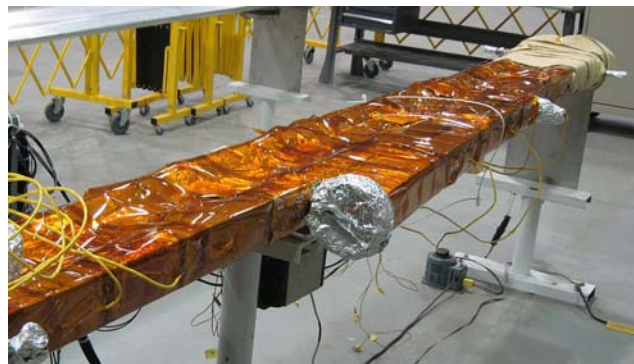


Figure 6 APS chamber bakeout development with the heater tapes positioned along the space between magnets with aluminum foil and Kapton foil wrapping.

The options of heater tape position and power density together with the thermal isolation options such as aluminium, kapton or duple kapton with aluminium coating were tested in many different configurations. Figure 7 shows some of the combinations of total power and thermal isolations that could be used. The final version will be optimized with the prototype of the multipole vacuum chamber mounted on the girder and within the magnets. There are other requirement that need to be full filled

such as maximum temperature over the heater tapes ($< 180\text{ }^{\circ}\text{C}$), heater tapes made of non-magnetic materials and radiation resistance.

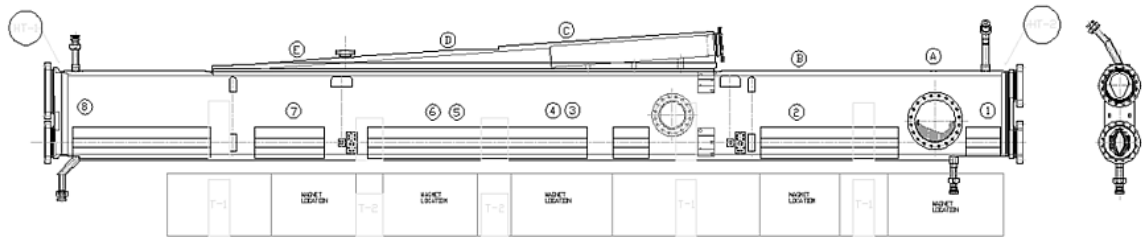
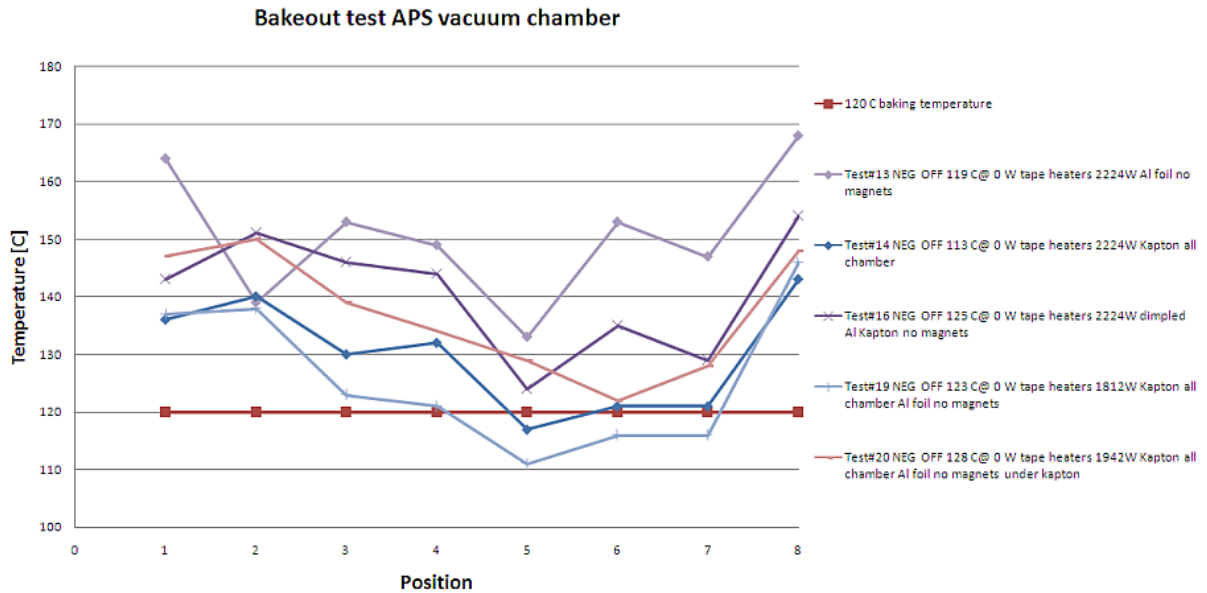


Figure 7. Temperature distributions along the chamber with some insulation options (upper) and the thermocouple position at the chamber (down).

6. RF shielded bellows

There are five aluminium chambers and two short stainless chambers in each DBA cell, connected to each other with RF-shielded bellows. There are RF-shielded bellows connecting the long straight section of insertion devices and of special components, such as RF cavities and injection devices, and damping wigglers. To reduce the broadband impedance of the vacuum chamber's wall and to minimize localized higher-order-mode (HOM) heating, the inner cross-section of the electron-beam chamber should be maintained as smooth as possible. High transverse impedance may induce beam instability, thereby putting an upper limit on the stored current. The changes in cross-sections of the beam chamber should vary smoothly, with an angle of inclination less than 10 degree for tapered transitions. The height of the steps should be less than 1 mm, in general, and less than 0.5 mm at small-aperture ducts for insertion devices. For the bellows, we will install RF contact fingers to reduce the impedance and provide a smooth path for the beam image current. The openings of the thin slits of these fingers should be such as to allow adequate pumping of the residual gases from behind the slits. Calculations to optimize the design of the thin slits while minimizing the impedance of the chambers give a loss factor of $\sim 1.0 \times 10^{-2}$ V/pC for each bellows. The design of the bellows uses the PEP-II [3] and SOLEIL[4] concept, with external finger contact, single spring-finger, and welded bellows, as shown in Figure 8. The magnetic permeability of welded bellows must be measured, since fast corrector magnets will be mounted at some bellows, another option could be the hydro formed bellows but with some decrease in flexibility.

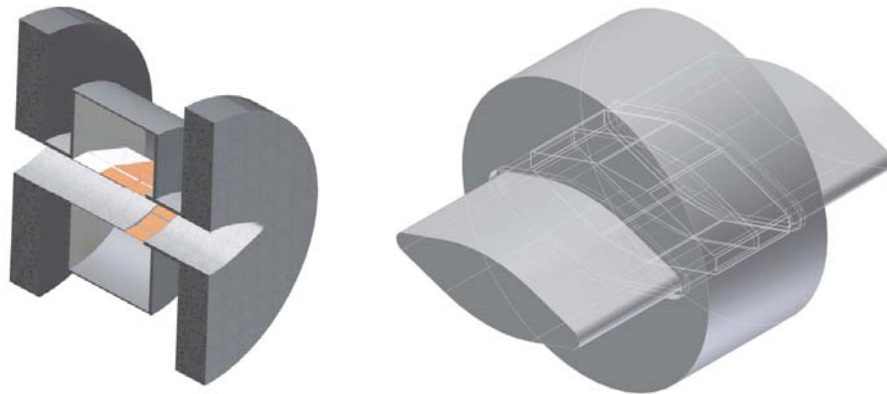


Figure 8. 3-D CAD model of sectional view of the RF-shielded bellows with single spring (left), and the model used for the loss factor simulation (right).

7. NEG strip support

Most of the NSLS-II storage ring's vacuum chambers will be fabricated from extruded aluminum and will be exposed to low levels of photon radiation from bending magnets or from insertion devices. The 25×76 mm electron beam channel will be vacuum pumped using distributed NEG strips in the antechamber connected by a narrow pumping slot, similar to those employed at others storage rings. This is deemed efficient to provide linear pumping to the beam channel through the opening of the photon exit. Dual strips will be mounted on the top and bottom of the antechamber. There will be sufficient clearance between the two mounted NEG strips to allow the passage of photons, even during mis-steering of the beam. The mounting of the dual strips, as shown in Figure 9, will be carefully designed and thoroughly tested to eliminate any potential electrical faults during the *in-situ* bake and NEG activation, as well as having a very flexible support for easy installation and maintenance in the tunnel. The NEG strip will be activated at 400 °C for 30 minutes by resistive heating with ~70 ampere current; which will be carried out at the end of the *in-situ* bakeout or during the period of machine maintenance.

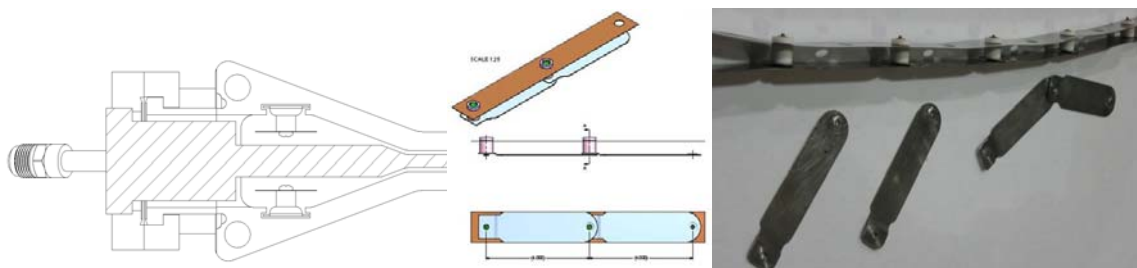


Figure 9. CAD cross section drawing of a NEG strip in the vacuum chamber (left), the model for the NEG support (centre), and the prototype sample for the installation test (right).

8. Summary

The construction of NSLS-II is to start in 2009 and ready for users in 2014. The NSLS-II storage ring vacuum chambers have been designed using proven, reliable and cost-effective technology. Most cell vacuum chambers will be fabricated from extruded aluminum. The details of the design of the chambers are complete. Test extrusion of both dipole and multipole chamber cross sections was successfully accomplished, and the machining and welding of the prototype chambers are underway. The development of the photon absorbers, the BPM, the bakeout process, the RF-shielded bellows and a versatile supports for the NEG strips, are also advancing rapidly, ready for the start of construction in early 2009.

9. Acknowledgments

This work was performed under auspices of the United States Department of Energy, under contract DE-AC02 98CH10886.

10. References

- [1] S.L. Kramer, et al. "NSLS-II Design: A Novel Approach to Light Source Design", Proc. 2007 Asian Particle Accel. Conf., Indore, India, pp613-15 (2007).
- [2] J. Noonan, J. Gagliano, G.A. Goepfner, R.A. Rosenberg, and D.R. Walters, "APS Storage Ring Vacuum System Performance," Proc. PAC97, p 3552-5 (1998).
- [3] M.E. Nordby, et al. "Bellows Design for the PEP-II High Energy Ring Arc Chamber", Proc. 1995 Particle Accel. Conf., Dallas, Texas, USA, pp2048-50 (1995).
- [4] M.P. Level, et al. "Progress Report on the Construction of SOLEIL", Proc. 2005 Particle Accel. Conf., Knoxville, Tennessee, USA, pp.2203-2205 (2005).